The EMBO Journal (2012) 31, 2378–2390 | © 2012 European Molecular Biology Organization | Some Rights Reserved 0261-4189/12
www.embojournal.org

THE EMBO JOURNAL

EMBO open

The location of splenic NKT cells favours their rapid activation by blood-borne antigen

Patricia Barral[1,2,*], María Dolores Sánchez-Niño[1], Nico van Rooijen[3], Vincenzo Cerundolo[2] and Facundo D Batista[1,*]

[1]Lymphocyte Interaction Laboratory, Cancer Research UK, London Research Institute, London, UK, [2]Medical Research Council Human Immunology Unit, Weatherall Institute of Molecular Medicine, John Radcliffe Hospital, Oxford, UK and [3]Department of Molecular Cell Biology, Faculty of Medicine, Vrije Universiteit, VUMC, Amsterdam, The Netherlands

Natural killer T (NKT) cells play an important role in mounting protective responses to blood-borne infections. However, though the spleen is the largest blood filter in the body, the distribution and dynamics of NKT cells within this organ are not well characterized. Here we show that the majority of NKT cells patrol around the marginal zone (MZ) and red pulp (RP) of the spleen. In response to lipid antigen, these NKT cells become arrested and rapidly produce cytokines, while the small proportion of NKT cells located in the white pulp (WP) exhibit limited activation. Importantly, disruption of the splenic MZ by chemical or genetic approaches results in a severe reduction in NKT cell activation indicating the need of cooperation between both MZ macrophages and dendritic cells for efficient NKT cell responses. Thus, the location of splenic NKT cells in the MZ and RP facilitates their access to blood-borne antigen and enables the rapid initiation of protective immune responses.

The EMBO Journal (2012) **31,** 2378–2390. doi:10.1038/emboj.2012.87; Published online 13 April 2012
Subject Categories: immunology
Keywords: blood-borne antigen; marginal zone; NKT cells

Introduction

NKT cells are a heterogeneous subset of classical αβ T lymphocytes that share the common characteristic of being restricted by the MHC class I-like molecule CD1, which can present self and foreign lipids (Barral and Brenner, 2007; Bendelac *et al*, 2007). As such, NKT cells can be directly activated in response to lipids from several bacteria (like *Shingomonas*, *Erlichia*, *Borrelia* or *Streptococcus*; Kinjo *et al*, 2005, 2006, 2011; Mattner *et al*, 2005) or in response to endogenous lipid antigens upregulated in antigen presenting cells (APCs) after TLR stimulation (Brigl *et al*, 2003; Paget *et al*, 2007; Salio *et al*, 2007). The activation of NKT cells by these two mechanisms explains their involvement in a broad range of immune responses against viruses, bacteria, fungus, anti-tumour immunity and autoimmune processes (Bendelac *et al*, 2007; Tupin *et al*, 2007; Cerundolo *et al*, 2009). Upon activation, NKT cells rapidly secrete large amounts of cytokines and induce downstream activation of different cell types, including dendritic cells (DCs), NK cells, B cells and conventional T cells. On this basis, NKT cells have been described as a bridge between innate and adaptive immune responses (Bendelac *et al*, 2007).

In recent years, various studies have highlighted the particular importance of NKT cells in responding to blood-borne pathogens and these cells have been shown to accumulate in the vasculature of both lung and liver (Geissmann *et al*, 2005; Velázquez *et al*, 2008; Lee *et al*, 2010; Scanlon *et al*, 2011). However, in spite of the fact that the spleen is the major site where immune responses to blood-borne antigens are initiated (Mebius and Kraal, 2005), little is currently understood about where NKT cells are located and their dynamic features in this organ. Indeed, due to the technical difficulties associated with unambiguous identification of these cells using immunohistochemistry (Berzins *et al*, 2005), the distribution of endogenous NKT cells in the spleen has remained an open question in the field.

The spleen is highly structured and composed of the red pulp (RP) that acts mainly as a blood filter, and the white pulp (WP) where the majority of B and T lymphocytes reside, separated by the marginal zone (MZ). The MZ contains a specialized subset of MZ B cells, DCs and two subsets of macrophages: MZ macrophages characterized by the expression of the surface receptors SIGN-R1 and/or MARCO (Elomaa *et al*, 1995; Geijtenbeek *et al*, 2002), and metallophilic macrophages expressing sialoadhesin (CD169, Siglec-1 (Kraal and Janse, 1986)). Arterial branches in the spleen terminate in the marginal sinus, allowing blood to transit through the MZ and into the RP (Mebius and Kraal, 2005). This organization allows cells in the MZ to be in continuous contact with blood-borne antigens and indeed, MZ B cells and macrophages have been described as main players in the initiation of immune responses against blood-borne pathogens (Martin *et al*, 2001; Aichele *et al*, 2003; Kang *et al*, 2004). The MZ is a very complex structure in which the various intercellular interactions appear to be critical for the organization and function of the individual cell types. However, the precise role of the MZ populations, particularly in antigen presentation during the initiation of immune responses, remains unclear (Ciavarra *et al*, 1997; Aichele *et al*, 2003; Backer *et al*, 2010; You *et al*, 2011).

Here, we have used a combination of pulse-labelling, immunofluorescence and multi-photon microscopy to show that the majority of splenic NKT cells localize to and patrol around the MZ and RP. In response to lipid antigen, these NKT

*Corresponding authors. P Barral, Lymphocyte Interaction Laboratory, Cancer Research UK, London Research Institute, 44 Lincoln's Inn Fields, London, WC2A 3LY, UK. Tel.: +44 (0)20 7269 3593; Fax: +44 (0)20 7269 3479; E-mail: patricia.barral@cancer.org.uk or FD Batista, Lymphocyte Interaction Laboratory, Cancer Research UK, London Research Institute, 44 Lincoln's Inn Fields, London, WC2A 3LY, UK. Tel.: +44 (0)20 7269 2059; Fax: +44 (0)20 7269 3479; E-mail: facundo.batista@cancer.org.uk

Received: 6 January 2012; accepted: 15 March 2012; published online: 13 April 2012

cells arrest in close proximity to antigen-containing cells in the MZ and become activated to secrete cytokines. In contrast, NKT cells located in the periarteriolar lymphoid sheath (PALS) showed limited activation. Moreover, the disruption of macrophages and dendritic cells in the MZ dramatically reduces NKT cell activation, suggesting that the cooperation of cells in the MZ is necessary for efficient NKT cell responses.

Results

NKT cells are highly accessible to the blood entering the spleen

Since the role of NKT cells in response to blood-borne antigen has been well established, we sought to examine the accessibility of NKT cells to the blood entering the spleen as an indication of their location. To do this, we adapted an *in vivo* pulse-labelling procedure that allows the selective labelling of cells according to their exposure to the blood (Figure 1; Cinamon *et al*, 2008; Pereira *et al*, 2009; Muppidi *et al*, 2011). Mice were intravenously (i.v.) injected with phycoerythrin-labelled anti-CD45 antibody (CD45-PE) and spleen sections were imaged by confocal microscopy (Figures 1A and B). As expected, the MZ region became highly labelled after a brief (3 min) exposure to CD45-PE, while no staining was detected in the WP that was protected from antibody arrival (Figure 1A). In line with this, flow cytometric analysis of the extent of CD45-PE labelling in total splenocytes revealed that a large proportion of MZ B cells ($B220^+CD21^{hi}CD23^{lo}$) were highly labelled with CD45-PE compared with follicular B ($B220^+CD21^{lo}CD23^{hi}$) and T cells (Figure 1A). Using this approach, we observed that the majority of splenic NKT cells, identified as either TCR-β^+αGalCer-CD1d tetramer$^+$B220$^-$ cells (Figure 1A) or TCR-β^+NK1.1$^+$B220$^-$ cells (Figure 1D), were highly labelled with CD45-PE (72 ± 7% and 75 ± 5%, respectively), indicating their proximity to the blood supplied to the spleen. Unlike MZ B cells, the proportion of NKT cells labelled after longer (20 min) antibody treatments remains stable (Figures 1B and C), although the mean fluorescence intensity (MFI) of labelling in the NKT population increased over time (Figure 1C). Interestingly, we did not observe striking phenotypical differences between highly and poorly *in vivo* labelled NKT cells in terms of the expression of CD4, CD8, DX5, CD44, CD122, NK1.1 and CD62L, although CD69 expression seemed to be higher in CD45-PE$^+$ NKT cells (Supplementary Figure S1).

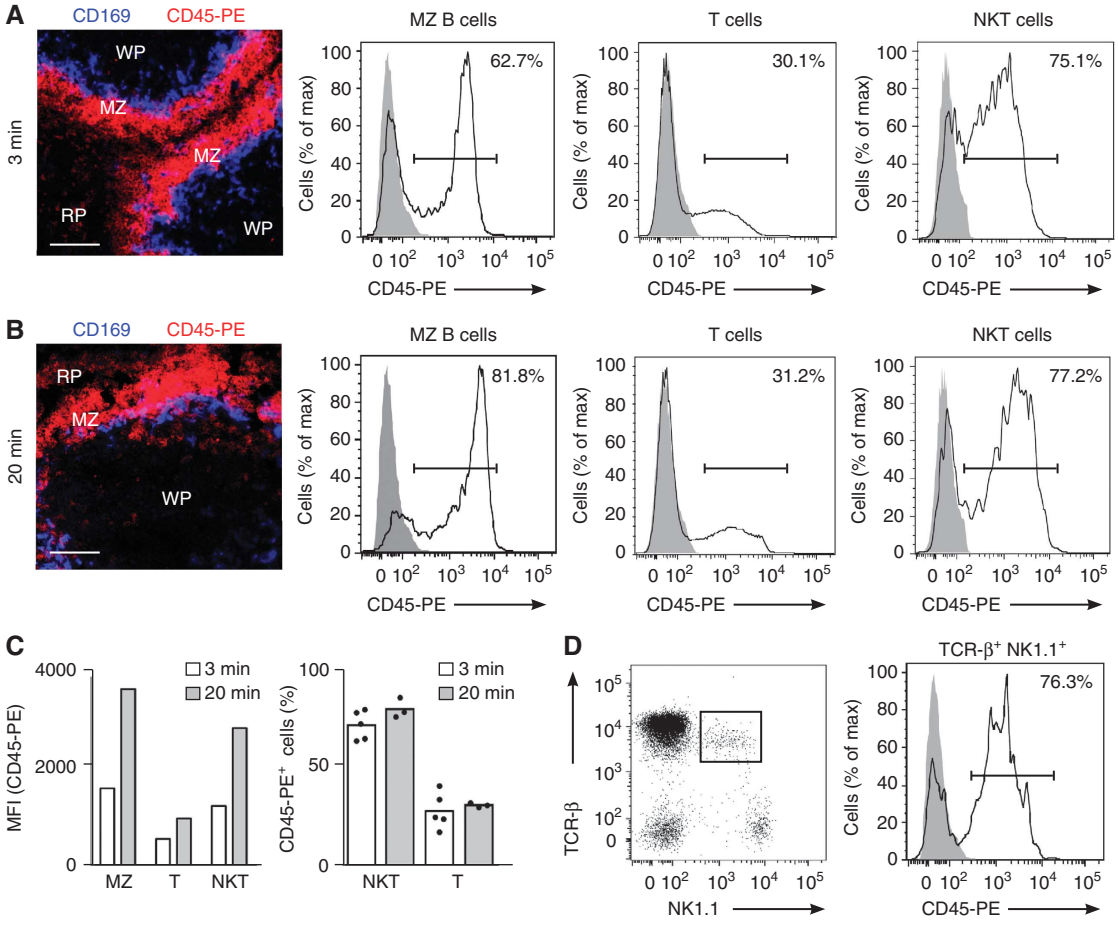

Figure 1 Splenic NKT cells are accessible to the blood entering the spleen. (**A**–**D**) Mice were injected with CD45-PE antibody 3 min (**A**, **C**, **D**) or 20 min (**B**, **C**) before analyses. (**A**, **B**) Immunofluorescence (left) from spleens of mice injected with CD45-PE (red) stained with CD169 (blue). Bars, 50 μm. Flow cytometry for CD45-PE binding by splenic MZ B cells, T cells and NKT cells (black line; grey solid profile, un-injected control) (**C**) MFI (left) and percentage of cells (right) binding to CD45-PE in the referred splenic populations at 3 and 20 min after injection. Each dot represents an individual animal. (**D**) Flow cytometry of B220$^-$ splenocytes showing TCR-β and NK1.1 (left), and binding of CD45-PE by TCR − β$^+$NK1.1$^+$B220$^-$ cells (right). Data represent 5 independent experiments with 2 mice per experiment.

Therefore, our results indicate that the majority of NKT cells are readily accessible to blood entering the spleen, suggesting that they reside outside the splenic WP.

NKT cells are preferentially located in the splenic MZ and RP

We moved on to directly visualize the distribution of endogenous NKT cells in the spleen and initially adopted an approach using CD1d tetramer staining of splenic frozen sections. However, consistent with previous reports, this proved technically challenging (Berzins *et al*, 2005; Thomas *et al*, 2011) and as a result of high levels of background staining we were unable to unambiguously identify endogenous NKT cells. To overcome this, we have used two alternative strategies to elucidate the distribution of splenic NKT cells. First, endogenous NKT cells were identified *in situ* in flash-frozen cryostat sections of spleens of mice previously perfused with neutral buffered formalin (Figures 2A and B; Supplementary Figure S2; Andrews *et al*, 2001). This method allows discrimination of TCR-β^+NK1.1$^+$ NKT cells from NK cells (NK1.1$^+$TCR-β^-) and conventional T cells (TCR-β^+NK1.1$^-$). However, as both TCR and NK1.1 can be down-regulated in activated NKT cells, we have used a second, complementary strategy involving the adoptive transfer of highly purified NKT cells into congenic recipients (Figures 2C and D; Supplementary Figure S2; Barral *et al*, 2010).

Importantly, both endogenous ($n=247$) and adoptively transferred ($n=81$) NKT cells occupied a similar distribution within the splenic sections. We observed that splenic NKT cells were predominantly located in the RP, MZ and T cell areas (47%, 25 and 23%, respectively) but virtually excluded from B cell follicles. In order to compare the relative distribution of NKT cells amongst splenic regions, the proportion of NKT cells was related to the cross-sectional area of each region (Supplementary Figures S2C and D, previously reported (Aoshi *et al*, 2008)). This type of analysis revealed the preferential accumulation of NKT cells in the MZ (Figures 2B and D). Notably, the total proportion of NKT cells present in the RP and MZ (~70%), and therefore readily accessible to the blood entering the spleen, is equivalent to the percentage of endogenous NKT cells labelled by *in vivo* antibody injection (Figure 1A). Similarly, the majority of adoptively transferred NKT cells were highly stained after pulse-labelling with CD45-PE (~72%), confirming that they occupy a similar distribution in the spleen than that of endogenous cells (Figure 2E).

To characterize the spatiotemporal dynamics of NKT cells in the spleen we have used time-lapse multi-photon microscopy. This method presents important technical difficulties since the maximum imaging depth achievable in the spleen is severely hampered by the absorption and scattering of light by blood. However, as the majority of NKT cells are excluded from the PALS, we imaged the spleen directly through the collagen capsule (to a maximum depth of 70 μm), which allowed us to visualize NKT cells outside the WP (Figures 2F–J, Supplementary Movies S1 and S2). Under these conditions, we observed that splenic NKT cells migrate with an average speed of 6.2 ± 2.7 μm/min (Figure 2G). The distribution of instantaneous speeds for NKT cells showed maximum values of around 20 μm/min and low arrest coefficients (13%) similar to those measured for conventional T cells (10%; Figures 2H and I). To visualize NKT cells located in deeper regions of the spleen (MZ and PALS) we performed an alternative imaging approach by cutting open the spleen across the transverse axis and placing the tissue in warm oxygenated medium for imaging (as previously reported (Aoshi *et al*, 2008; Bajénoff *et al*, 2008)). Under these imaging conditions NKT cells showed comparable dynamics to those of NKT cells visualized in intact spleen (average speed, 5.9 ± 0.4 μm/min; arrest coefficient, 13%; Supplementary Figure S3, Supplementary Movie S3).

Therefore, splenic NKT cells predominantly reside in the MZ and RP and patrol the resting spleen with similar dynamic features as those observed for conventional T cells.

NKT cells are activated by blood-borne lipid antigen outside the WP

The observed location of splenic NKT cells renders them in an ideal position to sense circulating antigen in its arrival to the spleen (Mebius and Kraal, 2005). Therefore we have used different approaches in order to investigate the behaviour of splenic NKT cells in response to antigen administration. To mimic conditions occurring during infection with bacteria encoding NKT cell agonists we injected mice i.v. with particles (200 nm diameter) coated with either α-linked galacturonic glycosphingolipid (GalA-GSL) from *Sphingomonas yanoikuyae* or αGalCer (Kinjo *et al*, 2005; Mattner *et al*, 2005; Barral *et al*, 2010).

We observed that the majority of splenic NKT cells were activated to produce IFN-γ and IL-4, within 2 h of i.v. injection with bacterial lipids (Figure 3A). A similar activation was observed following administration of particulate αGalCer while no cytokine production was detected after injection of control lipids (Figure 3A). Next we examined the distribution of both endogenous and adoptively transferred NKT cells 2 h after i.v. administration of lipid antigen (Figures 3B–D, Supplementary Figure S4A and B). At this time, we observed that the proportion of NKT cells in the splenic MZ increased (25 ± 4% to 38 ± 4%, $n=187$, Figures 3C and D). However, the total proportion of NKT cells outside the splenic WP did not significantly change following antigen administration (~70%, Figures 3C and D), suggesting that cells relocate from the RP into the splenic MZ.

Although the majority of NKT cells localize in the MZ after antigen administration still a number of cells remained in the WP. Therefore we sought to investigate a potential relationship between NKT cell location and their activation status by extending the *in vivo* pulse-labelling approach. Two hours after i.v. injection of particulate lipid antigen, mice received a 3 min pulse of CD45-PE and the extent of labelling was correlated with the activatory status of NKT cells (Figure 4). Notably, in response to either bacterial-derived GalA-GSL or αGalCer, the majority of NKT cells that were activated to secrete IL-4 and IFN-γ were highly labelled *in vivo* with CD45-PE. In contrast, those NKT cells located in the WP that were protected from CD45-PE labelling, exhibited very limited activation. Comparably, i.v. administration of soluble αGalCer induced the same kind of differential activation in NKT cells located inside or outside the splenic WP (Supplementary Figures S4C–F).

Thus, the localization of NKT cells outside the splenic WP promotes their early activation in response to blood-borne antigen arrival.

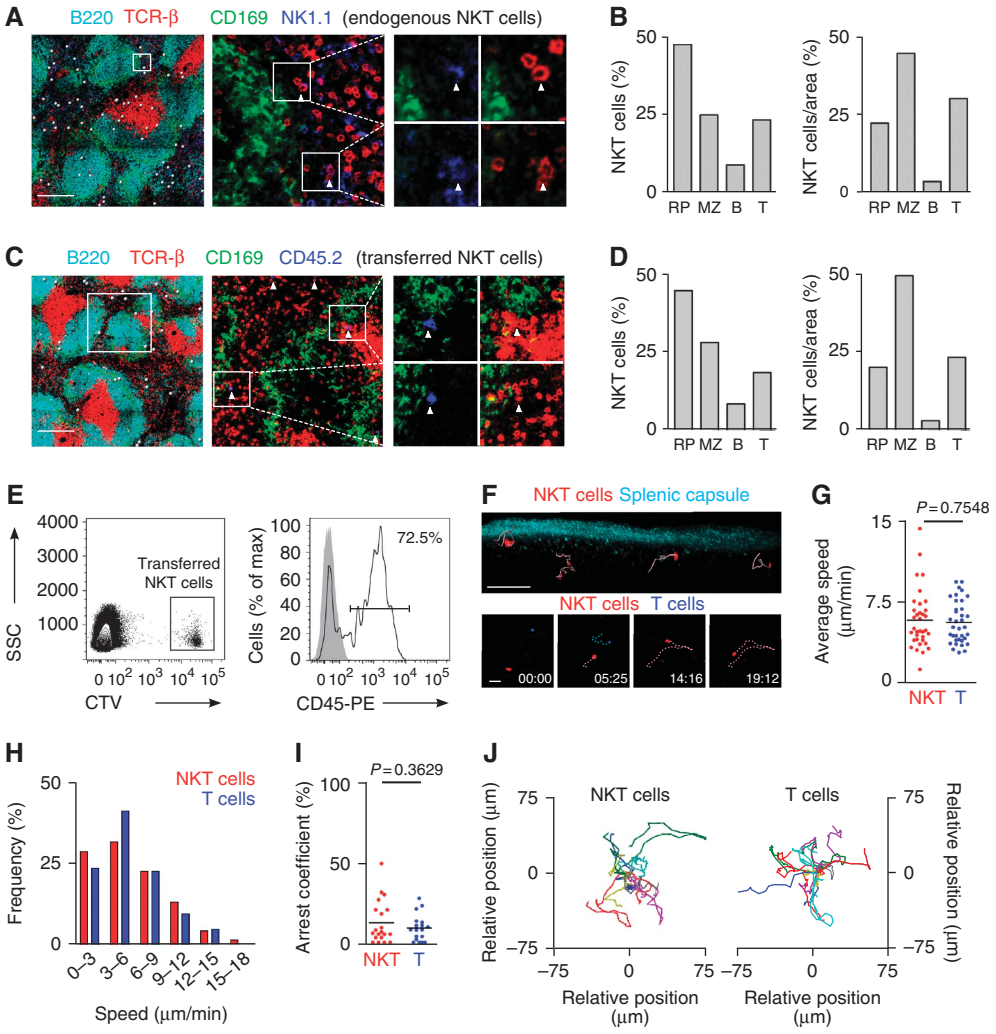

Figure 2 Splenic NKT cells are predominantly located in the MZ and RP. (**A–D**) Immunofluorescence from spleen sections stained with B220 (cyan), CD169 (green), TCR-β (red) and NK1.1 (blue, **A**) or CD45.2 (blue, **C**). White dots depict NKT cells. Bars, 200 μm. (**B**, **D**) Percentages (left) and proportion of cells per area (right) of NKT cells in the RP, MZ, B cell follicles (B) and PALS (T) for endogenous (**B**) and adoptively transferred (**D**) NKT cells. (**E**) 2×10^6 sorted NKT cells were labelled with CellTrace Violet (CTV) and injected into WT mice. 16 h later recipients were injected with CD45-PE 3 min before analysis. Transferred cells were detected in the recipient spleen as CTV^+ cells (left) and showed high CD45-PE labelling (right). (**F**, top) Multi-photon microscopy image of the spleen showing collagen capsule (blue) and NKT cells (red). Tracks for individual cells are depicted in pink. Bar, 50 μm. (**F**, bottom) Snapshot images showing NKT cells (red) and T cells (blue) at the indicated time points. Individual cell tracks are coloured in pink (NKT cells) and blue (T cells). Stamp, min:sec. Bars, 20 μm. (**G–J**) Average speed (**G**), speed distribution (**H**), arrest coefficient (**I**) and migratory tracks (**J**) for NKT cells and T cells. Each dot represents an individual cell. Data were pooled from 2 independent experiments with 2 mice each. *p*, unpaired two-tailed *t*-test.

Splenic NKT cells arrest in the MZ

Since NKT cell activation takes place within hours of antigen administration we asked the question of where blood-borne particulate lipids localized on their arrival to the spleen. The location of fluorescently labelled particulate lipids in the spleen was tracked using confocal microscopy of frozen sections (Figure 5A). Two hours after i.v. administration, lipid antigen was predominantly located in the MZ and co-localized with $MARCO^+$ and $SIGN\text{-}R1^+$ MZ macrophages and $CD11c^+$ DCs (Figure 5A). Importantly, we observed that endogenous NKT cells were also situated in the MZ and appeared in close proximity to cells containing particulate GalA-GSL and αGalCer (Figures 5B and C).

In order to understand the effect of antigen arrival in NKT cell dynamics we imaged the spleen by multi-photon microscopy 2 h after antigen administration. At this time point we observed that NKT cells stopped their migration and became confined in antigen-rich regions (Figures 5D–I, Supplementary Movies S4 and S5). Consequently we measured a decrease in the average speed of NKT cells (3.7 ± 2.5 μm/min versus 6.2 ± 2.7 μm/min in the absence of antigen; Figure 5E) that was accompanied by an increase in arrest coefficient (56% versus 13%; Figure 5H). In contrast, the average speed and arrest coefficient observed for conventional T cells was not changed following lipid antigen administration (6.2 ± 1.9 μm/min and 13.4%, respectively; Figures 5D–I). The alteration of the dynamic behaviour of splenic NKT cells in response to lipid antigen is similar to that reported for NKT cells both in lymph nodes and liver, suggesting that their migration provides a means of immune surveillance in tissues (Geissmann *et al*, 2005; Barral *et al*, 2010; Lee *et al*, 2010).

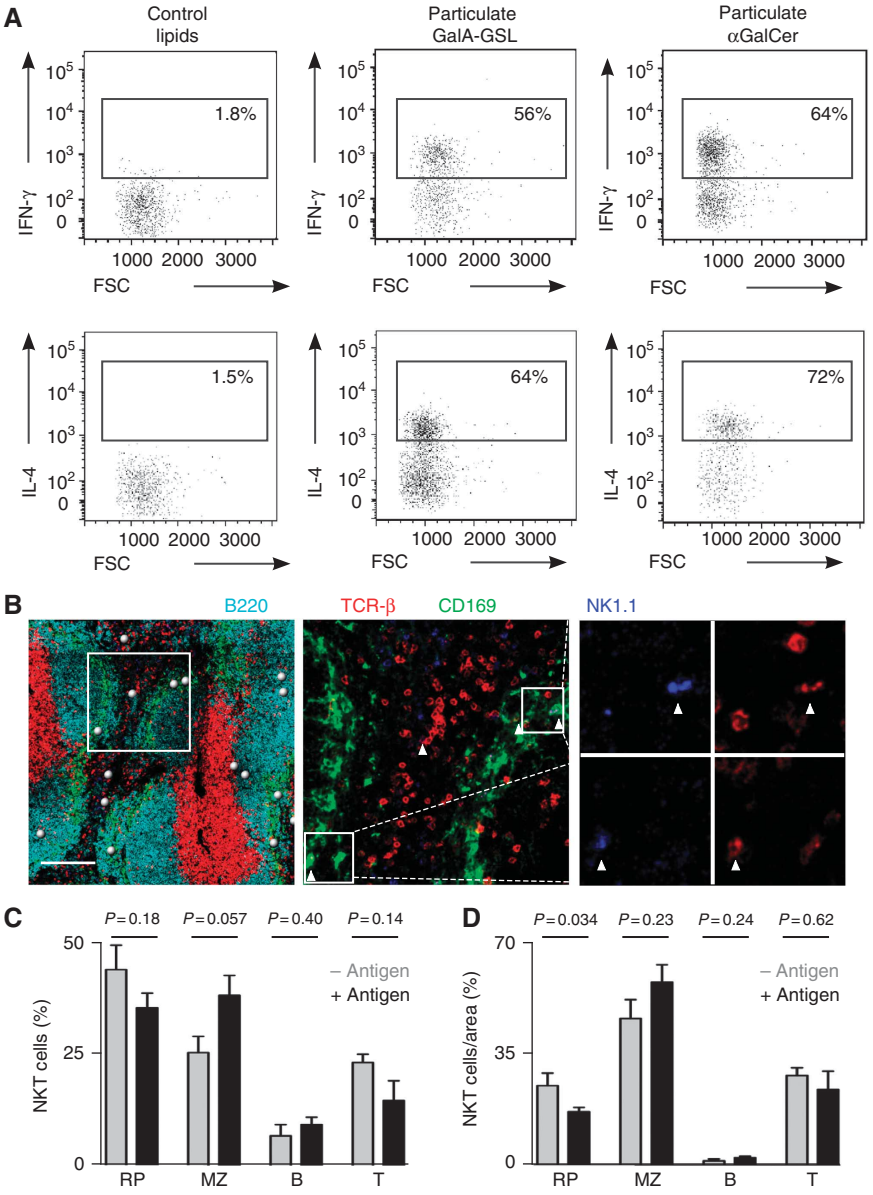

Figure 3 NKT cell activation in response to lipid antigen (**A**) Intracellular IFN-γ (top) and IL-4 (bottom) staining for splenic NKT cells (TCR-β$^+$αGalCer-CD1d tetramer$^+$B220$^-$) 2 h after injection of particulate control lipids (left), GalA-GSL (middle) or αGalCer (right). (**B**–**D**) Confocal microscopy identification of endogenous NKT cells 2 h after antigen injection. (**B**) Spleen sections were stained with B220 (cyan), CD169 (green), TCR-β (red) and NK1.1 (blue). Bars, 200 μm. (**C**, **D**) Percentages (**C**) and proportion of cells per area (**D**) for NKT cells in the RP, MZ, B cell follicles (B) and PALS (T). Data represent 2 independent experiments. *p*, unpaired two-tailed *t*-test.

Role of different APCs in activation of splenic NKT cells

The identity of the APCs that participate in the initiation of NKT cell activation in the spleen is largely unknown. To assess the ability of primary splenic DCs and MZ macrophages to retain lipid antigens arriving to the spleen we injected mice with fluorescent particulate lipids and 2 h later we analysed antigen retention by splenic cell populations by flow cytometry. At this time point around 50% of DCs and SIGN-R1$^+$ MZ macrophages were found to retain particulate lipids after *in vivo* injection (Figures 6A and B). Importantly, both of these cell types showed high expression of CD1d (Figures 6C and D).

Subsequently, we went on analysing the ability of MZ macrophages and DCs to stimulate NKT cell activation *in vitro*. To this end, SIGN-R1$^+$ macrophages and CD11c^{hi} DCs were enriched from splenic single cell suspensions by depletion of B and T cells and further purified by flow cytometry sorting (Figure 6E). After pre-incubation for 2 h with particulate lipids, sorted cells were co-cultured with NKT cell hybridoma DN32.D3 cells. As shown in Figure 6F αGalCer was efficiently presented by both DCs and SIGN-R1$^+$ cells, as measured by IL-2 production by DN32.D3 cells, with DCs showing a stronger presentation capacity than macrophages.

Thus, DCs and MZ macrophages retain lipid antigen on its arrival to the spleen and they can efficiently present lipids to mediate NKT cell activation.

NKT cell activation depends on the integrity of the MZ

To investigate the role of DCs and macrophages in mediating NKT cell activation *in vivo* we have used two different

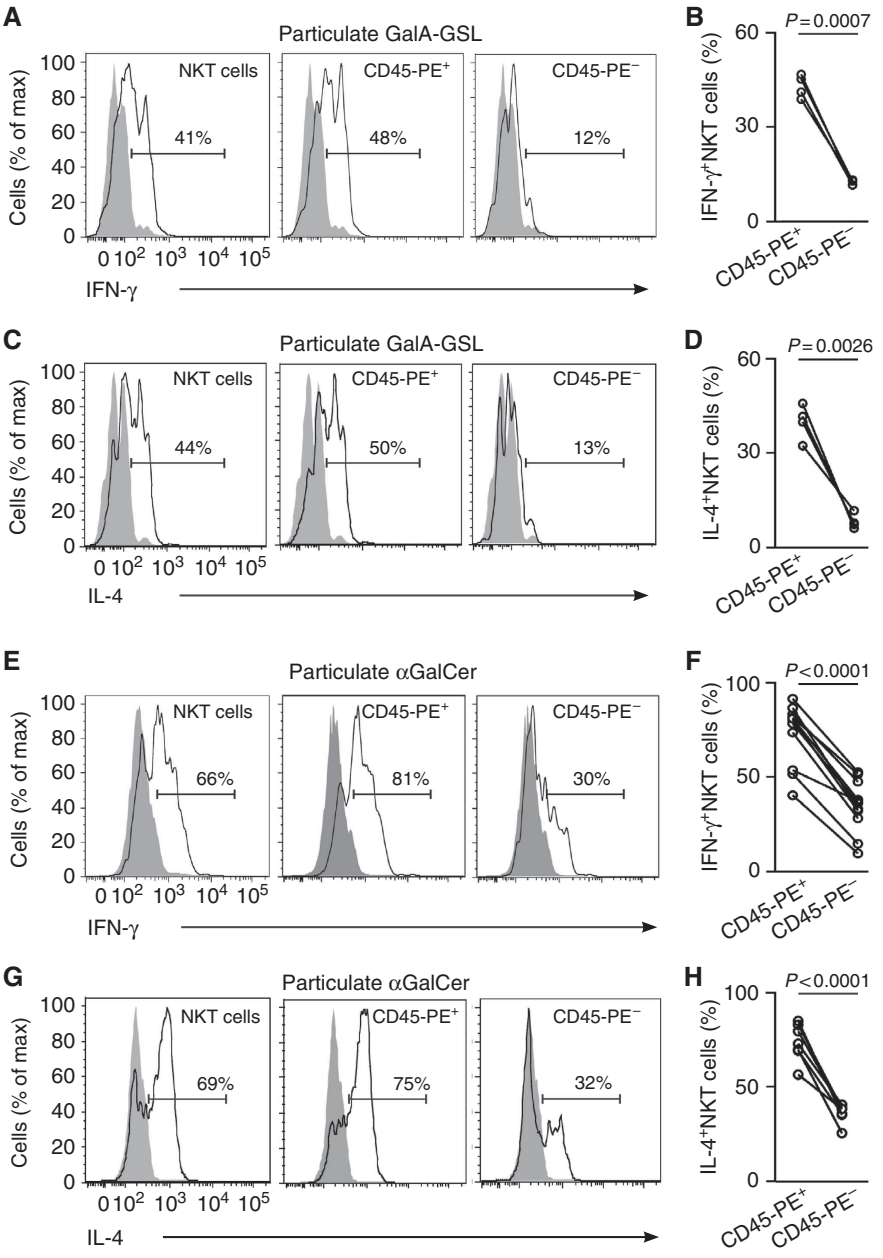

Figure 4 NKT cell activation occurs preferentially outside the WP. (**A**–**H**) Mice were injected with particulate GalA-GSL (**A**–**D**) or αGalCer (**E**–**H**) and 2 h later they received CD45-PE 3 min before analyses. Flow cytometry profiles and quantification of intracellular IFN-γ (**A**, **B** and **E**, **F**) and IL-4 (**C**, **D** and **G**, **H**) for total (left) and highly (middle, CD45-PE$^+$) or poorly (right, CD45-PE$^-$) CD45-PE labelled NKT cells (TCR-β$^+$αGalCer-CD1d tetramer$^+$B220$^-$). *p*, paired *t*-test. Data represent 3 independent experiments with at least 3 mice each.

approaches that allowed us to disrupt particular cell populations present in the spleen.

Firstly, mice were treated with clodronate liposomes (CLL) to selectively deplete macrophages in the MZ and RP. However, in line with previous reports (Aoshi *et al*, 2008), two days after CLL treatment we observed a depletion not only of MARCO$^+$, SIGN-R1$^+$, F4/80$^+$ and CD169$^+$ cells but also a reduction in CD11c^{hi} cells (Figure 7A, Supplementary Figure S5A–E). Concomitant with the loss of these cells, antigen was not efficiently retained in the splenic MZ and was instead dispersed throughout the RP. Moreover, at this time we detected a dramatic decrease in the percentage of NKT cells that were activated to secrete IFN-γ (23 ± 5% versus 69 ± 3%; Figure 7B, Supplementary Figure S5E), accompanied by a decrease in MFI for intracellular IFN-γ secreted by NKT cells (46 ± 13% MFI reduction after CLL treatment versus untreated mice).

As the DC population recovers more rapidly than macrophages after CCL administration, we went on to assess the contribution of these populations in NKT cell activation six days after CCL treatment which allows recovering of DCs while macrophages remain absent (Figures 7C and D, Supplementary Figure S5F–H). At this time, antigen was not efficiently retained at the MZ however we detected that a substantial proportion of NKT cells recovered their ability to secrete cytokines after antigen injection (46 ± 9% IFN-γ$^+$ NKT cells; 28 ± 18% MFI reduction for IFN-γ after CLL treatment versus untreated mice; Figure 7D, Supplementary

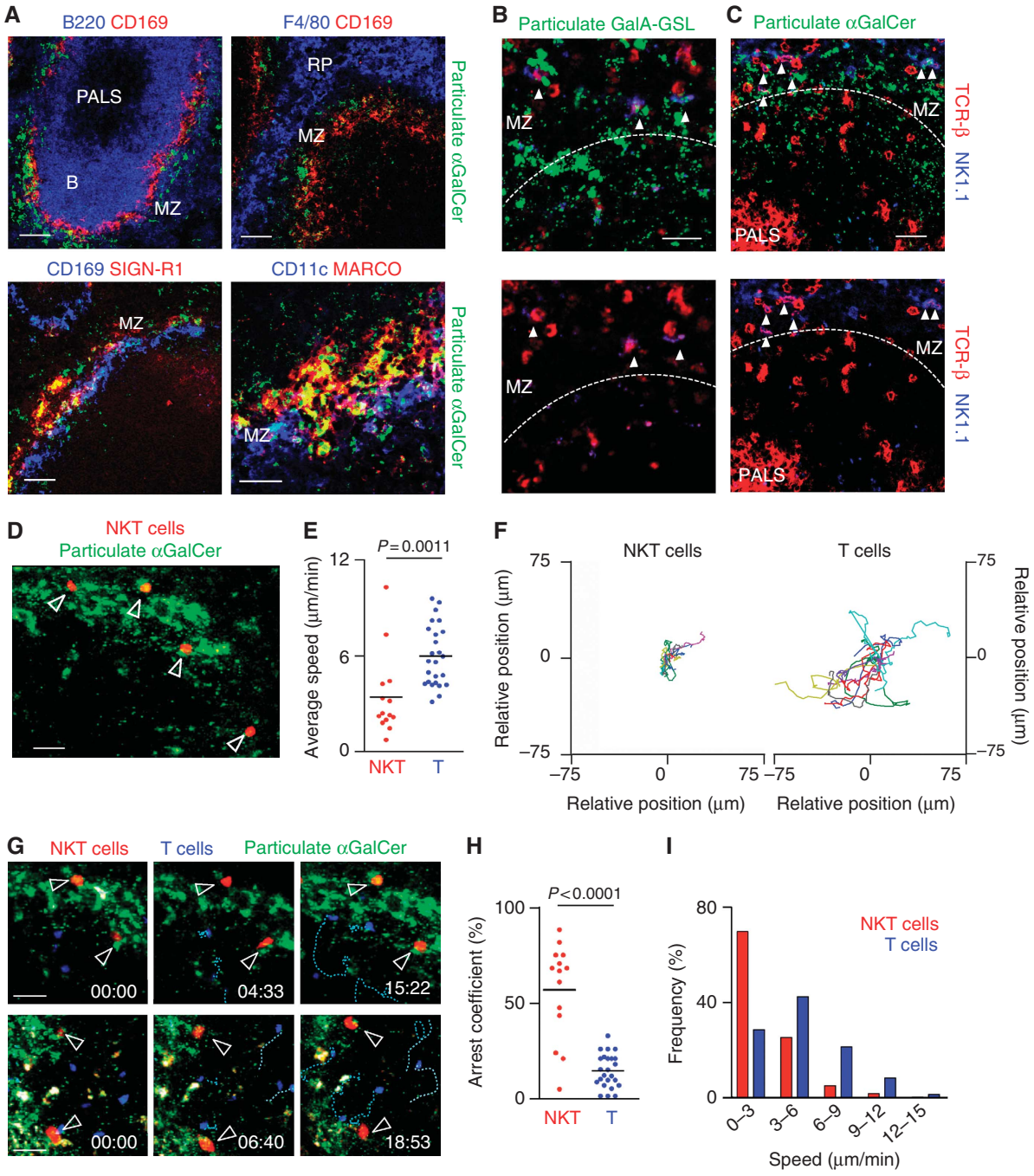

Figure 5 NKT cells arrest in the MZ in response to lipid antigen. (**A–C**) Mice received lipid antigen 2 h before analyses. (**A**) Immunofluorescence of spleen sections showing particulate αGalCer (green) stained with CD169, SIGN-R1 or MARCO (red) and B220, CD11c or F4/80 (blue). (**B**, **C**) Immunofluorescence of spleen sections showing particulate GalA-GSL (**B**, green) and αGalCer (**C**, green) and endogenous NKT cells stained with TCR-β (red) and NK1.1 (blue). Bars, 50 μm. (**D–I**) NKT cell dynamics after antigen administration. Mice were injected with particulate αGalCer (green) 2 h before imaging. (**D**) Multi-photon microscopy image of the spleen showing particulate lipids (green) and NKT cells (red). Average speed (**E**), migratory tracks (**F**), snapshot images (**G**), arrest coefficient (**H**) and speed distribution (**I**) for splenic NKT cells (red) and T cells (blue). Individual cell tracks are coloured in pink (NKT cells) and blue (T cells). Bars, 20 μm. *p*, unpaired two-tailed *t*-test. Data were pooled from 2 independent experiments with 2 mice each.

Figure S5H), suggesting that DCs play a significant role in mediating NKT cell activation. At later times after CLL treatment (16 days) we found that DC numbers were equivalent to those of WT mice and the populations of F4/80$^+$ and MARCO$^+$ macrophages started to recover, with cells appearing scattered through the RP and partially colocalizing with injected particulate lipids (Figures 7E and F, Supplementary Figure S5I–K). However CD169$^+$ and SIGN-R1$^+$ cells remained absent (Supplementary Figure S5I). Despite the reappearance of some macrophage populations, the extent of NKT cell activation after antigen injection (41 ± 4% IFN-γ NKT cells, Figure 7F) was still comparable to the one measured at 6 days after CLL treatment suggesting that the positioning of the different macrophage populations in the

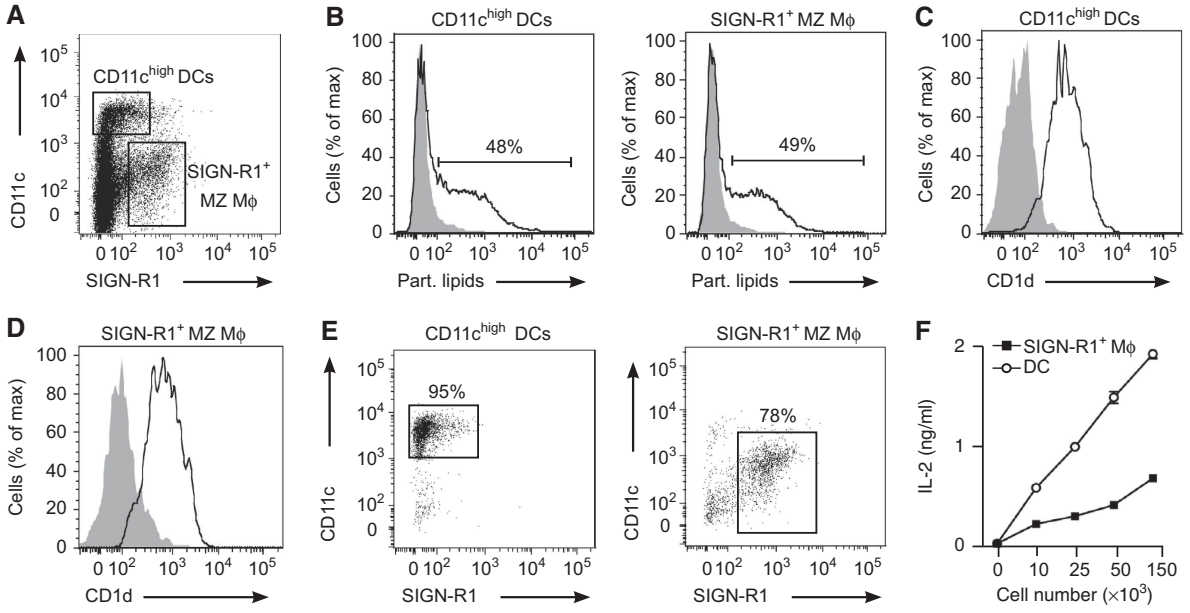

Figure 6 Role of different APCs in NKT cell activation (**A**) Flow cytometry analyses of splenic single cell suspensions showing CD11c^{high} DC and SIGN-R1$^+$ macrophage populations. (**B**) Flow cytometry analyses of lipid uptake by CD11c^{high} DCs (left) and SIGN-R1$^+$ macrophages (right) in the spleen 2 h after injection of αGalCer particles (un-injected control, grey filled histogram). (**C**, **D**) CD1d expression in splenic DCs (**C**) and SIGN-R1$^+$ macrophages (**D**). (**E**) DCs (left) and SIGN-R1$^+$ macrophages (right) were purified by sorting and stained with CD11c and SIGN-R1 antibodies. (**F**) Lipid presentation by sorted DCs (O) and SIGN-R1$^+$ MZ macrophages (■) incubated with αGalCer particles previous to co-culture with DN32.D3 NKT cells. Secretion of IL-2 into the culture medium by DN32.D3 cells was measured as a read-out for lipid presentation.

MZ is important for efficient antigen retention and subsequent NKT cell activation. Twenty two days after CLL treatment we observed a complete recovery of all macrophage populations, accompanied by an efficient antigen retention in the MZ and full recovery of NKT cell activation (60 ± 4% IFN-γ NKT cells; Figures 7G and H).

Finally, to further delineate the cellular requirements for splenic NKT cell activation, we took advantage of the CD11c-DOG model that allows depletion of CD11c$^+$ cells after injection of diphtheria toxin (DT; Hochweller *et al*, 2008). Two days after DT treatment, we observed not only complete ablation of DCs, but also depletion of both MZ and RP macrophages while the population of MZ B cells didn't appear to change substantially (Figure 7I; Supplementary Figure S5L–O; Hochweller *et al*, 2008). This depletion was accompanied by a reduction in antigen retention at the MZ and a dramatic decrease in NKT cell activation following lipid administration (23 ± 2%; Figures 7I and J; Supplementary Figure S5L-N). Intriguingly, even in the absence of DCs and macrophages, around 20% of NKT cells were activated to secrete IFN-γ suggesting that other APCs such as B cells may also participate in NKT cell activation in the spleen.

Discussion

In this study we show that the majority of splenic NKT cells are located in the MZ and RP, with only a small proportion of cells located in the WP. Shortly after administration, lipid antigens were retained in the MZ by macrophages and DCs, where they trigger NKT cell activation. In contrast, NKT cells located in the PALS have restricted access to antigen and therefore exhibit limited secretion of cytokines. Disruption of macrophages and DCs within the MZ compartment reduces the extent of NKT cell activation, suggesting that these populations cooperate to trigger effective NKT cell responses.

Despite the fact that the spleen is one of the preferential locations for NKT cells in the body, the distribution and dynamics of NKT cells in this organ have remained unclear because of the technical difficulties often associated with unambiguous identification of NKT cells *in situ* and limited imaging depth possible in this blood-rich organ (Berzins *et al*, 2005; Aoshi *et al*, 2008; Bajénoff *et al*, 2010). Recently CD1d tetramer staining has been used to visualize NKT cells in the spleen of Vα14 transgenic mice, with cells appearing located mainly in the PALS (Thomas *et al*, 2011). However in line with our observations, the authors were unable to unambiguously identify individual splenic NKT cells in WT mice by tetramer staining. To overcome this we have used two complementary strategies to examine the location of both endogenous and adoptively transferred NKT cells. By using these two approaches we confirmed the presence of a proportion of NKT cells in the PALS (~30%) though the majority of NKT cells appear scattered around the MZ and RP of the spleen. In steady-state conditions, NKT cells patrol the spleen with an average speed of around 6.2 μm/min, similar to that observed for CD8$^+$ T cells in the WP (~5 μm/min; Aoshi *et al*, 2008). These speeds are slower than those reported for equivalent cells in lymph nodes (Aoshi *et al*, 2008; Barral *et al*, 2010) suggesting that the environmental differences between tissues might affect the cell motility. Since NKT cells are located in blood-rich regions of the spleen we cannot discard that the lack of blood flow in splenic explants may lead to alterations in cell behaviour. However the data obtained so far for lymphocyte dynamics in

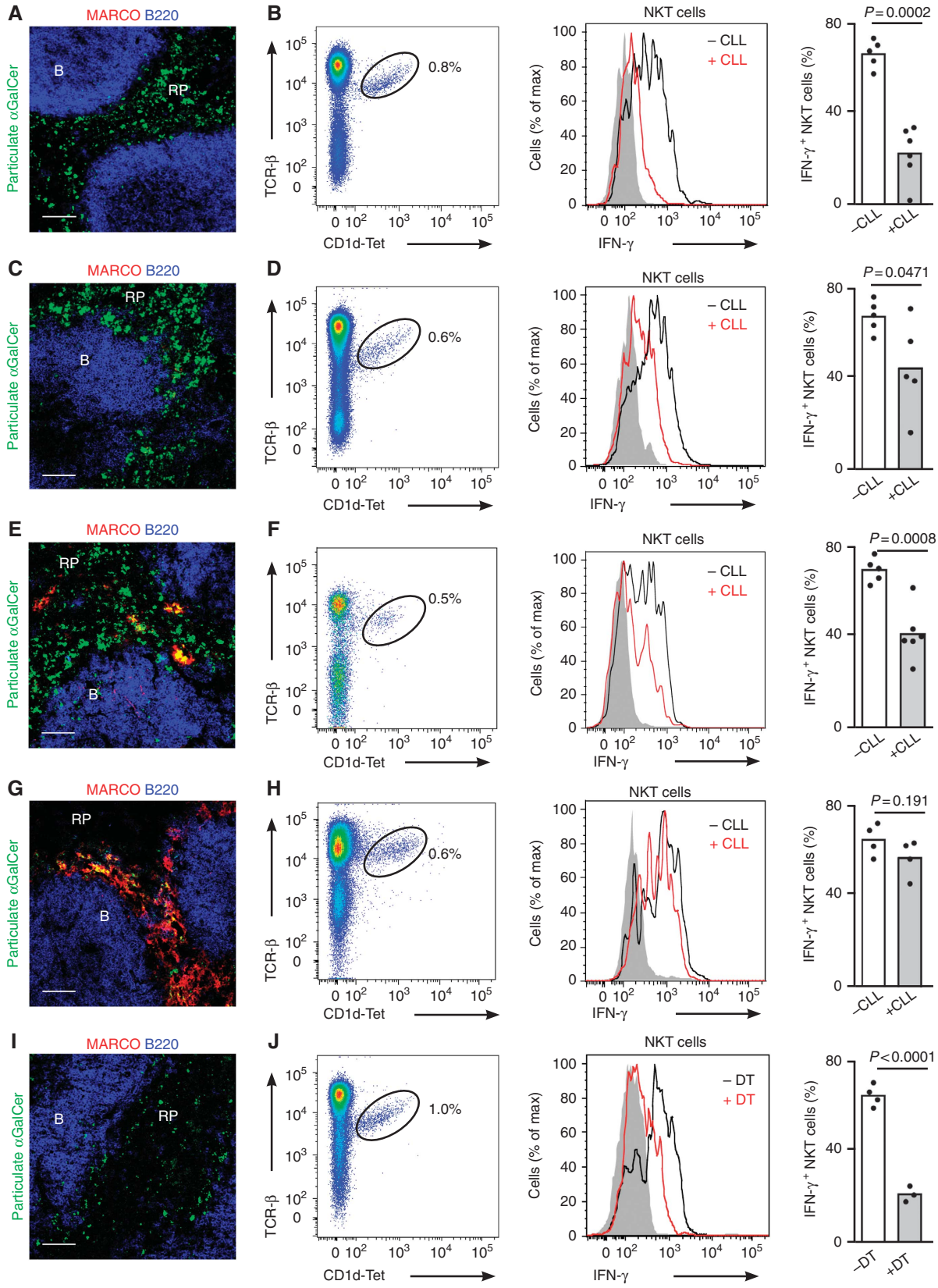

Figure 7 Disruption of the MZ reduces NKT cell activation. (**A**–**J**) Mice were injected with particulate αGalCer 2 h before analyses. Confocal microscopy images (**A**, **C**, **E**, **G**, **I**) and flow cytometry profiles (**B**, **D**, **F**, **H**, **J**) of spleens from WT mice treated with CLL for 2 days (**A**, **B**), 6 days (**C**, **D**), 16 days (**E**, **F**) or 22 days (**G**, **H**) and CD11c-DOG mice treated with DT (**I**, **J**). Immunofluorescence images show particulate αGalCer (green), MARCO (red) and B220 (blue); Bars, 50 μm. Flow-cytometry plots show NKT cells (left), intracellular IFN-γ staining for NKT cells (middle) and quantification of IFN-γ production (right) for NKT cells in treated (+) and untreated (−) mice. *p*, unpaired two-tailed *t*-test. Data represent 2 independent experiments with at least 3 mice per experiment.

explanted organs correlates with the results obtained using intra-vital microscopy of surgically exposed tissues (Huang *et al*, 2004).

The observed distribution of splenic NKT cells has important implications for our understanding of how these cells are involved in mounting responses to blood-borne antigen. Indeed the continuous exposure of MZ cells to bacterial and viral antigens in the circulation facilitates rapid responses and successful control of infection (Mebius and Kraal, 2005). As such, the location of the majority of NKT cells in close proximity to blood entering the spleen facilitates the rapid encounter of patrolling NKT cells with antigen. In concert, as NKT cells typically present an activated/memory-like phenotype this ensures very rapid secretion of cytokines after antigen encounter, promoting protective responses. In line with this suggestion, lung and liver NKT cells have also been detected in an intravascular location, which may allow the rapid sensing of blood-borne antigens in those tissues (Geissmann *et al*, 2005; Velázquez *et al*, 2008; Lee *et al*, 2010).

The localization of NKT cells in the MZ might also play a role in the initiation of rapid adaptive immune responses. Like NKT cells, MZ B cells have been implicated in early immune responses, as they are responsible for the first wave of antibody secretion in response to bacterial antigen (Martin *et al*, 2001) and mediate more rapid responses against blood-borne viral particles compared with follicular B cells (Gatto *et al*, 2004). Interestingly, MZ B cells express higher levels of CD1d than follicular B cells and are more efficient than follicular B cells in presenting antigen to NKT cells (Galli *et al*, 2003; Barral *et al*, 2008; Leadbetter *et al*, 2008; Chang *et al*, 2012; King *et al*, 2012). Moreover it has been recently suggested that interactions between MZ B cells and NKT cells might play a role *in vivo* to boost CD1-dependent immune responses (Muppidi *et al*, 2011). Indeed, many bacteria contain repetitive epitopes in their surface and/or lipid antigens that can favour internalization by specific MZ B cells and subsequent interaction with splenic NKT cells to allow early antibody responses.

Traditionally the location of effector T cells has been examined by visualizing their spatial distribution in static snapshots of tissues. Though informative, such approaches provide little information as to the relationship between location and effector function. To overcome these limitations, we used a combination of multi-photon microscopy, flow cytometry and immunohistochemistry to examine where splenic NKT cell activation occurs *in vivo*. In response to lipid antigen, we observed that concomitant with rapid activation to secrete cytokines, splenic NKT cells became arrested in close proximity to antigen-containing cells, a common feature associated with T cell activation (Cahalan and Parker, 2008). Importantly, activation was more evident in NKT cells in close proximity to blood entering the spleen, suggesting that antigen presentation occurs predominantly outside the WP. Interestingly, we obtained similar NKT cell activation pattern upon injection of soluble lipids. This is probably due to the association of blood-borne αGalCer with apolipoproteins forming lipid transport particles that will not have access to the splenic conduit system and will therefore be retained in the MZ (Nolte *et al*, 2003; van den Elzen *et al*, 2005; Barral and Brenner, 2007). NKT cell activation in the MZ resembles the response of memory $CD8^+$ T cells that cluster in the MZ and RP early in response to infection (Bajénoff *et al*, 2010; Kurachi *et al*, 2011). In contrast, it has been reported that the activation of conventional T cells takes place mainly in the PALS during bacterial infection (Khanna *et al*, 2007; Aoshi *et al*, 2008). In this scenario, DCs transport bacteria from the MZ into the PALS and present antigen to specific $CD8^+$ T cells, though this takes place over several hours (Aoshi *et al*, 2008). Thus it seems that antigen presentation occurs in various regions of the spleen, the precise location presumably is dependent on the nature of the antigen, the timing of the response and the different cell types involved.

The splenic MZ is a complex environment in which a plethora of interactions among different cell types are required for its function and maintenance. To understand the role that MZ organization plays in NKT cell activation, we have used genetic and chemical approaches to deplete various cellular populations in the MZ. Though CCL are widely used to deplete macrophages (Van Rooijen and Sanders, 1994), it has been reported that other populations might be affected very soon after CCL treatment (Aoshi *et al*, 2008) and in line with this we observed a decrease in the number of $CD11c^{high}$ DCs. Perhaps unsurprisingly, disruption of both macrophages and DCs results in a dramatic decrease in NKT cell activation. However, at later times after substantial recovery of the DC population, there was a partial rescue of NKT cell activation after antigen administration. To further investigate the emerging role of DCs in NKT cell activation, we took advantage of the CD11c-DOG system that allows depletion of DCs after administration of DT (Probst *et al*, 2005; Hochweller *et al*, 2008). However, as the depletion of DCs in this system was accompanied by the concomitant disappearance of splenic macrophages, we were unable to definitively identify whether a unique population was responsible for presenting antigen to NKT cells. Nevertheless, taken together our findings suggest that the cooperation of both macrophages and DCs may be necessary to achieve efficient NKT cell responses. In line with this, several studies support the idea that the cross talk between DCs and macrophages promotes efficient T cell responses (Aichele *et al*, 2003; Backer *et al*, 2010; You *et al*, 2011). Although DCs appear to play a major role in antigen presentation to splenic T cells, they are not absolutely required as macrophages can act as substitutes in their absence (Neuenhahn *et al*, 2006). Moreover in view of the fact that MZ macrophages mediate efficient antigen retention (Aichele *et al*, 2003; Kang *et al*, 2004) it has been proposed that they might retain antigen in the spleen and transfer it to DCs to initiate efficient T cell responses (Backer *et al*, 2010). Intriguingly, even in the absence of DCs and macrophages, we detected a significant NKT cell activation in response to blood-borne antigen indicating that other APCs such as B cells may also participate in NKT cell activation in the spleen.

In conclusion, we have shown that the majority of NKT cells are located in the MZ and RP, rendering them accessible to blood-borne antigen and thereby facilitating their rapid activation. As NKT cells have been implicated in a wide variety of immune responses, such as following infection or anti-tumour immunity, our observations provide new insight into the regulation of NKT cell-mediated immune responses that could lead to the design of improved vaccination strategies.

Materials and methods

Antigens, lipid preparation and microsphere coating

αGalCer was purchased from Enzo Life Sciences. GalA-GSL was kindly provided by Dr Mitchell Kronenberg (Division of Cell Biology, La Jolla Institute for Allergy and Immunology, La Jolla, CA 92037, USA). 1,2-Dioleoyl-sn-Glycero-3-Phosphocholine (DOPC) was purchased from Avanti Polar Lipids. Liposomes containing DOPC/αGalCer (90/10, w/w) or DOPC/GalA-GSL (90/10, w/w) were prepared as described (Barral *et al*, 2010). For coating, silica microspheres (200nm diameter; Kisker GbR) were incubated with liposomes for 10 min, washed with PBS containing 1% BSA (Sigma) and 1% FCS (Gibco-Invitrogen) and resuspended in PBS.

Mice, cell lines and injections

Vα14 TCR transgenic, CD11c-DOG, CD45.1 C57BL/6 and C57BL/6 WT mice were bred and maintained at the animal facility of Cancer Research UK or the John Radcliffe Hospital, Oxford. All experiments were approved by the Cancer Research UK, Animal Ethics Committee and the United Kingdom Home Office.

1–10 μl stock of particles ($\sim 10^9$ particles/μl) were resuspended in 200 μl PBS for i.v. injection. For CLL treatment mice were i.p. injected with a standard suspension clodronate-loaded liposomes 2, 6, 16 or 22 days before analysis. Clodronate was a gift of Roche Diagnostics GmbH. Other reagents for preparation of liposomes (Van Rooijen and Sanders, 1994) were phosphatidylcholine (LIPOID E PC; Lipoid GmbH) and cholesterol (Sigma).

For cell depletion in CD11c-DOG, mice were injected i.p. twice with DT (8 ng/gram body weight) 48 h before analyses (Hochweller *et al*, 2008).

NKT hybridoma DN32.D3 was kindly provided by A. Bendelac (University of Chicago, Chicago, IL).

Flow cytometry analysis of in vivo antibody labelling and NKT cell activation

For *in vivo* antibody labelling experiments, mice were i.v. injected with 2 μg of anti-mouse CD45-PE or CD45-FITC antibody (104; eBioscience) and sacrificed for tissue analyses 3 or 20 min after injection. Single-cell spleen suspensions for flow cytometry were obtained by mincing the tissue through a 70 μm strainer followed by erythrocyte lysis. Flow cytometry analyses were performed in FACS buffer containing PBS, 1% BSA and 1% FCS. Anti-mouse CD16/32 (2.4G2, BD Biosciences) was used to block non-specific antibody binding. Afterwards the following directly labelled anti-mouse antibodies were used: B220-pacific blue (RA3-6B2), TCR-β – APCCy7 (H57-597), CD44-PECy5 (IM7) from BD Biosciences; CD69-PE (H1.2F3) and CD122-PE (5H4) from eBioscience; CD4-PE (GK1.5; Biolegend); CD8-PB (5H10; Caltag), and αGalCer loaded-CD1d tetramer-APC (ProImmune). Anti-mouse CD21-FITC (7G6, BD Biosciences) and anti-mouse CD23-APC (2G8, Southern Biotech) were used to identify MZ and follicular B cells. Dead cells were excluded from the analysis by staining with DAPI (2-(4-Amidinophenyl)-6-indolecarbamidine dihydrochloride, Sigma).

For intracellular IFN-γ and IL-4 staining single cell suspension were prepared and stained with B220-pacific blue, TCR-β-APC-Cy7 and αGalCer loaded-CD1d tetramer-APC prior to fixation and permeabilization with Cytofix/Cytoperm solutions (BD Biosciences). Fixed cells were stained with anti-mouse IFN-γ-FITC (XMG1.2, BD Biosciences) or anti-IL-4-AlexaFluor 488 (11B11, BD Biosciences). All data were collected on an LSRFortessa flow cytometer (Becton Dickinson) and were analysed with FlowJo software (TreeStar).

Isolation of DCs and SIGN-R1$^+$ macrophages, in vitro lipid presentation assays and ELISA for IL-2

For purification of splenic DCs and SIGN-R1$^+$ macrophages single-cell spleen suspensions were prepared by treatment with collagenase IV and DNase I for 30 min at 37C and mincing the tissue through a 70 μm strainer followed by erythrocyte lysis. B and T cells were depleted by using Mouse Pan B and Pan T Dynabeads (Invitrogen) prior to sorting with CD11c-FITC (HL3, BD Biosciences) and SIGN-R1-Alexa 647 (22D1, eBioscience) antibodies.

For analysis of αGalCer presentation, sorted cells were incubated for 2 h with 1 μl of particles, washed 3 times and cultured ($1–15 \times 10^4$ cells/well) with 5×10^4 cells/well of DN32.D3 cells for 16 h in 96 well U-bottom plates with 200 μl of RPMI 1640 with 10% FCS. IL-2 concentration was determined by a standard sandwich ELISA in the supernatant of the culture medium, using anti-IL-2 (JES6-1A12) antibody for capture and biotinylated anti-IL-2 (JES6-5H4) antibody for detection (both BD Pharmingen).

Isolation of NKT cells and adoptive transfer

NKT cells were purified by sorting from the spleen of Vα14 TCR transgenic mice as previously described (Barral *et al*, 2010). Purity of the sample was confirmed to be higher than 95% by staining with αGalCer loaded-CD1d tetramer-APC. $2–3 \times 10^6$ purified NKT cells were injected by tail vein injection in 4–6 week old C57BL/6 CD45.1 congenic recipients. For some experiments purified NKT cells were labelled with SNARF-1 (Invitrogen) or CellTrace Violet (CTV, Invitrogen) before transfer. After 16–20 h recipients were injected i.v. with 5 μl of the stock of particulate lipids ($\sim 10^9$ particles/μl) or with 2 μg of anti-mouse CD45-PE.

Immunofluorescence

For staining of endogenous TCR-β$^+$NK1.1$^+$ NKT cells mice were under terminal anaesthesia and perfused with 10% neutral buffered formalin before removal of the spleen for cryosections. Cryostat sections (10 μm thick) of spleen were blocked with PBS containing 1% BSA and 10% goat serum for 30 min prior to incubation with pacific-blue rat anti-mouse B220 (RA3-6B2, BD Biosciences), TCR-β – PE (H57-597), CD169-FITC (3D6.112, AbDSerotec) and NK1.1-APC (PK136, eBioscience). For detection of adoptively transferred NKT cells the following antibodies were used: B220-pacific blue (RA3-6B2, BD Biosciences), TCR-β – PE (H57-597), CD169-FITC (3D6.112, AbDSerotec) and CD45.2-APC (104, BD Biosciences).

Alternatively, sections were incubated with the following anti-mouse antibodies: B220-Alexa 647 (RA3-6B2, BD Biosciences), F4/80-Alexa 647 (CI:A3-1, Biolegend), B220-FITC (RA3-6B2, BD Biosciences), CD169-FITC (3D6.112, AbDSerotec), MARCO-FITC (ED31, AbDSerotec), SIGNR1-Alexa 647 (22D1, eBioscience) and hamster anti-mouse CD11c (N418, Caltag), followed by Alexa 647-conjugated goat anti-hamster IgG (Molecular Probes) and Alexa 488-conjugated anti-flourescein/Oregon green rabbit IgG (Molecular Probes) when FITC-labelled antibodies were used. Imaging was carried out on a LSM 710s (Zeiss) inverted confocal microscope.

Multi-photon microscopy imaging of the spleen

$2–3 \times 10^6$ purified NKT cells were labelled with SNARF-1 and injected by tail vein injection in 4–6 weeks old WT recipients together with the same number of CMAC labelled T cells. For multi-photon microscopy imaging, spleens were attached to the base of a glass-bottom 35 mm culture dish by veterinary topical tissue adhesive and were continuously perfused with warmed (37 °C) RPMI 1640 medium without Phenol Red (GIBCO, Invitrogen) and bubbled with carbogen (95% O_2, 5% CO_2). For imaging of deep spleen regions, thick sections of fresh spleen (1–2 mm) were obtained by transversally cutting the tissue with a sharp scalpel (as previously reported (Khanna *et al*, 2007)). Sections were glued to a culture dish on the resected surface and perfused with warmed oxygenated medium as described above. The system was set up inside the environmental chamber that covers the microscope, maintaining a temperature of 37 °C throughout the imaging session. Image acquisition was performed with an upright multi-photon microscope (Olympus Fluoview FV1000 MPE2 Twin system) using a water-immersion 25×1.05 NA objective (Olympus XLPLNWMP) and a pulsed Ti:sapphire laser (Spectra Physics MaiTai HP DeepSee) tuned to provide an excitation wavelength of 800 nm. For four-dimensional imaging (x, y, z, and time), stacks of 11–20 square xy planes spanning 508 μm by 508 μm with 5 μm z spacing were acquired over 20–30 min (30–40 time-points). Emission wavelengths were detected through 420–500 nm (CMAC), 515–560 nm (green fluorescent particles) and 590–650 nm (SNARF-1) band-pass filters. Sequences of image stacks were transformed into volume-rendered four-dimensional movies and analysed with Imaris 6.3×64 software (Bitplane).

Data analysis

Analysis of four-dimensional multi-photon movies was performed using Imaris 6.3×64 software (Bitplane). The average speed of individual cells was calculated as path length over time (μm/min). Arrest coefficient was calculated as the percentage of each track in which the cell moved more slowly than 2 μm/min. The x, y and z

coordinates from individual cell tracks were obtained with Imaris. Tracks normalized at the same departure point were plotted with MatLab (The Mathworks Inc.).

Supplementary data
Supplementary data are available at *The EMBO Journal* Online (http://www.embojournal.org).

Acknowledgements

This work was funded by: Cancer Research UK (FDB and PB); Royal Society Wolfson Research Merit Award (FDB); Cancer Research UK (C399/A2291 and C5255/A10339; VC), The Wellcome Trust (Programme Grant 084923 VC, FDB and PB), the seventh European Community Framework Programme (Marie Curie Intra-European Fellowship, PIEF-GA-2008-220863; PB) and Instituto de Salud Carlos III (postdoctoral fellowship FIS-Sara Borrell and RETIC REDINREN 06/0016, MDSN). We thank Mitchell Kronenberg (La Jolla Institute for Allergy & Immunology) for providing GalA-GSL and for helpful comments on the manuscript; GJ Hämmerling, and N Garbi (Institute of Experimental Immunology; Institutes of Molecular Medicine and Experimental Immunology; Germany) and Caetano Reis e Sousa and Neil Rogers (Cancer Research UK) for CD11c-DOG mice. We also would like to thank the members of the Lymphocyte Interaction Lab for helpful comments and discussions.

Conflict of interest

The authors declare that they have no conflict of interest.

References

Aichele P, Zinke J, Grode L, Schwendener RA, Kaufmann SHE, Seiler P (2003) Macrophages of the splenic marginal zone are essential for trapping of blood-borne particulate antigen but dispensable for induction of specific T cell responses. *J Immunol* **171:** 1148–1155

Andrews DM, Farrell HE, Densley EH, Scalzo AA, Shellam GR, Degli-Esposti MA (2001) NK1.1+ cells and murine cytomegalovirus infection: what happens in situ? *J Immunol* **166:** 1796–1802

Aoshi T, Zinselmeyer BH, Konjufca V, Lynch JN, Zhang X, Koide Y, Miller MJ (2008) Bacterial entry to the splenic white pulp initiates antigen presentation to CD8+ T cells. *Immunity* **29:** 476–486

Backer R, Schwandt T, Greuter M, Oosting M, Jungerkes F, Tuting T, Boon L, O'toole T, Kraal G, Limmer A, Den Haan JMM (2010) Effective collaboration between marginal metallophilic macrophages and CD8+ dendritic cells in the generation of cytotoxic T cells. *Proceedings of the National Academy of Sciences* **107:** 216–221

Bajénoff M, Glaichenhaus N, Germain RN (2008) Fibroblastic reticular cells guide T lymphocyte entry into and migration within the splenic T cell zone. *J Immunol* **181:** 3947–3954

Bajénoff M, Narni-Mancinelli E, Brau F, Lauvau G (2010) Visualizing early splenic memory CD8+ T cells reactivation against intracellular bacteria in the mouse. *PLoS ONE* **5:** e11524

Barral DC, Brenner MB (2007) CD1 antigen presentation: how it works. *Nat Rev Immunol* **7:** 929–941

Barral P, Eckl-Dorna J, Harwood NE, De Santo C, Salio M, Illarionov P, Besra GS, Cerundolo V, Batista FD (2008) B cell receptor-mediated uptake of CD1d-restricted antigen augments antibody responses by recruiting invariant NKT cell help in vivo. *Proc Natl Acad Sci USA* **105:** 8345–8350

Barral P, Polzella P, Bruckbauer A, Van Rooijen N, Besra GS, Cerundolo V, Batista FD (2010) CD169(+) macrophages present lipid antigens to mediate early activation of iNKT cells in lymph nodes. *Nat Immunol* **11:** 303–312

Bendelac A, Savage PB, Teyton L (2007) The biology of NKT cells. *Annu Rev Immunol* **25:** 297–336

Berzins SP, Smyth MJ, Godfrey DI (2005) Working with NKT cells—pitfalls and practicalities. *Curr Opin Immunol* **17:** 448–454

Brigl M, Bry L, Kent SC, Gumperz JE, Brenner MB (2003) Mechanism of CD1d-restricted natural killer T cell activation during microbial infection. *Nat Immunol* **4:** 1230–1237

Cahalan MD, Parker I (2008) Choreography of cell motility and interaction dynamics imaged by two-photon microscopy in lymphoid organs. *Annu Rev Immunol* **26:** 585–626

Cerundolo V, Silk J, Masri SH, Salio M (2009) Harnessing invariant NKT cells in vaccination strategies. *Nat Rev Immunol* **9:** 28–38

Chang P-P, Barral P, Fitch J, Pratama A, Ma CS, Kallies A, Hogan JJ, Cerundolo V, Tangye SG, Bittman R, Nutt SL, Brink R, Godfrey DI, Batista FD, Vinuesa CG (2012) Identification of Bcl-6-dependent follicular helper NKT cells that provide cognate help for B cell responses. *Nature Immunology* **13:** 35–43

Ciavarra RP, Buhrer K, Van Rooijen N, Tedeschi B (1997) T cell priming against vesicular stomatitis virus analyzed in situ: red pulp macrophages, but neither marginal metallophilic nor marginal zone macrophages, are required for priming CD4+ and CD8+ T cells. *J Immunol* **158:** 1749–1755

Cinamon G, Zachariah MA, Lam OM, Foss FW, Cyster JG (2008) Follicular shuttling of marginal zone B cells facilitates antigen transport. *Nat Immunol* **9:** 54–62

Elomaa O, Kangas M, Sahlberg C, Tuukkanen J, Sormunen R, Liakka A, Thesleff I, Kraal G, Tryggvason K (1995) Cloning of a novel bacteria-binding receptor structurally related to scavenger receptors and expressed in a subset of macrophages. *Cell* **80:** 603–609

Galli G, Nuti S, Tavarini S, Galli-Stampino L, De Lalla C, Casorati G, Dellabona P, Abrignani S (2003) CD1d-restricted help to B cells by human invariant natural killer T lymphocytes. *J Exp Med* **197:** 1051–1057

Gatto D, Ruedl C, Odermatt B, Bachmann MF (2004) Rapid response of marginal zone B cells to viral particles. *J Immunol* **173:** 4308–4316

Geijtenbeek TBH, Groot PC, Nolte MA, van Vliet SJ, Gangaram-Panday ST, van Duijnhoven GCF, Kraal G, van Oosterhout AJM, van Kooyk Y (2002) Marginal zone macrophages express a murine homologue of DC-SIGN that captures blood-borne antigens in vivo. *Blood* **100:** 2908–2916

Geissmann F, Cameron T, Sidobre S, Manlongat N, Kronenberg M, Briskin M, Dustin M, Littman D (2005) Intravascular immune surveillance by CXCR6+ NKT cells patrolling liver sinusoids. *PLoS Biol* **3:** e113

Hochweller K, Striegler J, Hämmerling GJ, Garbi N (2008) A novel CD11c.DTR transgenic mouse for depletion of dendritic cells reveals their requirement for homeostatic proliferation of natural killer cells. *Eur J Immunol* **38:** 2776–2783

Huang AYC, Qi H, Germain RN (2004) Illuminating the landscape of in vivo immunity: insights from dynamic in situ imaging of secondary lymphoid tissues. *Immunity* **21:** 331–339

Kang Y-S, Kim JY, Bruening SA, Pack M, Charalambous A, Pritsker A, Moran TM, Loeffler JM, Steinman RM, Park CG (2004) The C-type lectin SIGN-R1 mediates uptake of the capsular polysaccharide of Streptococcus pneumoniae in the marginal zone of mouse spleen. *Proc Natl Acad Sci USA* **101:** 215–220

Khanna KM, McNamara JT, Lefrançois L (2007) In situ imaging of the endogenous CD8 T cell response to infection. *Science* **318:** 116–120

King IL, Fortier A, Tighe M, Dibble J, Watts GFM, Veerapen N, Haberman AM, Besra GS, Mohrs M, Brenner MB, Leadbetter EA (2012) Invariant natural killer T cells direct B cell responses to cognate lipid antigen in an IL-21-dependent manner. *Nature Immunology* **13:** 44–50

Kinjo Y, Illarionov P, Vela JL, Pei B, Girardi E, Li X, Li Y, Imamura M, Kaneko Y, Okawara A, Miyazaki Y, Gómez-Velasco A, Rogers P, Dahesh S, Uchiyama S, Khurana A, Kawahara K, Yesilkaya H, Andrew PW, Wong C-H *et al* (2011) Invariant natural killer T cells recognize glycolipids from pathogenic Gram-positive bacteria. *Nat Immunol* **12:** 966–974

Kinjo Y, Tupin E, Wu D, Fujio M, Garcia-Navarro R, Benhnia MR, Zajonc DM, Ben-Menachem G, Ainge GD, Painter GF, Khurana A, Hoebe K, Behar SM, Beutler B, Wilson IA, Tsuji M, Sellati TJ, Wong CH, Kronenberg M (2006) Natural killer T cells recognize diacylglycerol antigens from pathogenic bacteria. *Nat Immunol* **7:** 978–986

Kinjo Y, Wu D, Kim G, Xing GW, Poles MA, Ho DD, Tsuji M, Kawahara K, Wong CH, Kronenberg M (2005) Recognition of bacterial glycosphingolipids by natural killer T cells. *Nature* **434:** 520–525

Kraal G, Janse M (1986) Marginal metallophilic cells of the mouse spleen identified by a monoclonal antibody. *Immunology* **58:** 665–669

Kurachi M, Kurachi J, Suenaga F, Tsukui T, Abe J, Ueha S, Tomura M, Sugihara K, Takamura S, Kakimi K, Matsushima K (2011) Chemokine receptor CXCR3 facilitates CD8 + T cell differentiation into short-lived effector cells leading to memory degeneration. *J Exp Med* **208:** 1605–1620

Leadbetter, Brigl, Illarionov, Cohen, Luteran, Pillai, Besra, Brenner (2008) NK T cells provide lipid antigen-specific cognate help for B cells. *Proc Natl Acad Sci USA* **105:** 8339–8344

Lee W-Y, Moriarty TJ, Wong CHY, Zhou H, Strieter RM, van Rooijen N, Chaconas G, Kubes P (2010) An intravascular immune response to Borrelia burgdorferi involves Kupffer cells and iNKT cells. *Nat Immunol* **11:** 295–302

Martin F, Oliver AM, Kearney JF (2001) Marginal zone and B1 B cells unite in the early response against T-independent blood-borne particulate antigens. *Immunity* **14:** 617–629

Mattner J, Debord KL, Ismail N, Goff RD, Cantu C, Zhou D, Saint-Mezard P, Wang V, Gao Y, Yin N, Hoebe K, Schneewind O, Walker D, Beutler B, Teyton L, Savage PB, Bendelac A (2005) Exogenous and endogenous glycolipid antigens activate NKT cells during microbial infections. *Nature* **434:** 525–529

Mebius RE, Kraal G (2005) Structure and function of the spleen. *Nat Rev Immunol* **5:** 606–616

Muppidi JR, Arnon TI, Bronevetsky Y, Veerapen N, Tanaka M, Besra GS, Cyster JG (2011) Cannabinoid receptor 2 positions and retains marginal zone B cells within the splenic marginal zone. *J Exp Med* **208:** 1941–1948

Neuenhahn M, Kerksiek KM, Nauerth M, Suhre MH, Schiemann M, Gebhardt FE, Stemberger C, Panthel K, Schröder S, Chakraborty T, Jung S, Hochrein H, Rüssmann H, Brocker T, Busch DH (2006) CD8alpha + dendritic cells are required for efficient entry of Listeria monocytogenes into the spleen. *Immunity* **25:** 619–630

Nolte MA, Belien JAM, Schadee-Eestermans I, Jansen W, Unger WWJ, van Rooijen N, Kraal G, Mebius RE (2003) A conduit system distributes chemokines and small blood-borne molecules through the splenic white pulp. *Journal of Experimental Medicine* **198:** 505–512

Paget C, Mallevaey T, Speak AO, Torres D, Fontaine J, Sheehan KC, Capron M, Ryffel B, Faveeuw C, Leite de Moraes M, Platt F, Trottein F (2007) Activation of invariant NKT cells by toll-like receptor 9-stimulated dendritic cells requires type I interferon and charged glycosphingolipids. *Immunity* **27:** 597–609

Pereira JP, An J, Xu Y, Huang Y, Cyster JG (2009) Cannabinoid receptor 2 mediates the retention of immature B cells in bone marrow sinusoids. *Nat Immunol* **10:** 403–411

Probst HC, Tschannen K, Odermatt B, Schwendener R, Zinkernagel RM, Van Den Broek M (2005) Histological analysis of CD11c-DTR/GFP mice after in vivo depletion of dendritic cells. *Clin Exp Immunol* **141:** 398–404

Salio M, Speak AO, Shepherd D, Polzella P, Illarionov PA, Veerapen N, Besra GS, Platt FM, Cerundolo V (2007) Modulation of human natural killer T cell ligands on TLR-mediated antigen-presenting cell activation. *Proc Natl Acad Sci USA* **104:** 20490–20495

Scanlon ST, Thomas SY, Ferreira CM, Bai L, Krausz T, Savage PB, Bendelac A (2011) Airborne lipid antigens mobilize resident intravascular NKT cells to induce allergic airway inflammation. *J Exp Med* **208:** 2113–2124

Thomas SY, Scanlon ST, Griewank KG, Constantinides MG, Savage AK, Barr KA, Meng F, Luster AD, Bendelac A (2011) PLZF induces an intravascular surveillance program mediated by long-lived LFA-1-ICAM-1 interactions. *J Exp Med* **208:** 1179–1188

Tupin E, Kinjo Y, Kronenberg M (2007) The unique role of natural killer T cells in the response to microorganisms. *Nat Rev Microbiol* **5:** 405–417

van den Elzen P, Garg S, León L, Brigl M, Leadbetter E, Gumperz J, Dascher C, Cheng T, Sacks F, Illarionov P, Besra G, Kent S, Moody D, Brenner M (2005) Apolipoprotein-mediated pathways of lipid antigen presentation. *Nature* **437:** 906–910

Van Rooijen N, Sanders A (1994) Liposome mediated depletion of macrophages: mechanism of action, preparation of liposomes and applications. *J Immunol Methods* **174:** 83–93

Velázquez P, Cameron TO, Kinjo Y, Nagarajan N, Kronenberg M, Dustin ML (2008) Cutting edge: activation by innate cytokines or microbial antigens can cause arrest of natural killer T cell patrolling of liver sinusoids. *J Immunol* **180:** 2024–2028

You Y, Myers RC, Freeberg L, Foote J, Kearney JF, Justement LB, Carter RH (2011) Marginal zone B cells regulate antigen capture by marginal zone macrophages. *The Journal of Immunology* **186:** 2172–2181

